THE SOLAR NEIGHBORHOOD. XVIII. DISCOVERY OF NEW PROPER MOTION STARS WITH 0''.40 yr $^{-1}>\mu \geq 0$ ''.18 yr $^{-1}$ BETWEEN DECLINATIONS -90° and -47°

Charlie T. Finch, Todd J. Henry, John P. Subasavage, and Wei-Chun Jao Georgia State University, Atlanta, GA 30302-4106

Nigel C. Hambly

Scottish Universities Physics Alliance (SUPA), Institute for Astronomy, University of Edinburgh

Royal Observatory, Blackford Hill, Edinburgh, EH9 3HJ, Scotland, UK

finch@chara.gsu.edu

ABSTRACT

We report 1606 new proper motion systems in the southern sky (declinations -90° to -47°) with 0'.40 yr⁻¹ > $\mu \geq 0$ '.18 yr⁻¹. This effort is a continuation of the SuperCOSMOS-RECONS (SCR) proper motion search to lower proper motions than reported in Papers VIII, X, XII, and XV in this series. Distance estimates are presented for the new systems, assuming that all stars are on the main sequence. We find that 31 systems are within 25 pc, including two systems — SCR 0838-5855 and SCR 1826-6542 — we anticipate to be within 10 pc. These new discoveries constitute a more than ten-fold increase in new systems found in the same region of sky searched for systems with $\mu \geq 0$ '.40 yr⁻¹, suggesting a happy hunting ground for new nearby slower proper motion systems in the region just north (declinations -47° to 0°), much of which has not been rigorously searched during previous efforts.

Subject headings: solar neighborhood — stars: distances — stars: statistics — surveys — astrometry

1. INTRODUCTION

In this new edition of the investigation of the solar neighborhood, we continue the search for nearby stars by focusing our efforts on systems with proper motions between 0.40 yr⁻¹

and 0″.18 yr⁻¹. The likelihood that a slow proper motion system is nearby is far lower than a fast proper motion system. Nonetheless, the much larger number of slow proper motion systems discovered provides an extensive dataset for Galactic structure analyses, yields many candidates for followup work, and reveals a few nearby gems that move little relative to the Sun.

The pioneering surveys of (Giclas et al. 1971, 1978) and (Luyten 1979, 1980)¹ have provided most of the proper motion systems catalogued, even as massive computer searches of digitized photographic plates have become possible. The comprehensive New Luyten Two-Tenths catalogue (NLTT) contains 58693 proper motion objects with $\mu > 0''.18 \text{ yr}^{-1}$. Since then, many new high proper motion surveys have been carried out using new techniques, each of which compliments the work of Giclas and Luyten. In chronological order, surveys that sampled the sky south of declination -47° (the region relevant to the survey reported here) include (1) seven papers covering various portions of the southern sky by Wroblewski and collaborators who used photographic plates (Wroblewski & Torres 1994), (2) UKST survey plates of 40 survey fields by Scholz and collaborators (Scholz et al. 2000, 2002), (3) a survey of the South Galactic Cap down to $R_{59F} = 19.8$ (Oppenheimer et al. 2001), (4) the machine-selected catalogue of 11289 objects from SuperCOSMOS R-band material generated by (Pokorny et al. 2004), (5) our own SuperCOSMOS-RECONS (SCR) proper motion search of the entire southern sky (Hambly et al. 2004; Henry et al. 2004; Subasavage et al. 2005a,b), which uses plates with all four emulsions, (6) the southern infrared proper motion survey (SIPS) (Deacon et al. 2005), which uses a combination of Two Micron All Sky Survey (2MASS) data and SuperCOSMOS I band images, and (7) Lepine's SUPERBLINK survey of a portion of the southern sky (Lépine 2005). The Calan-ESO survey (Ruiz et al. 2001), which identified proper motions in 14 ESO areas of the southern sky, did not reach as far south as declination -47° (but one of the three ESO regions in (Ruiz et al. 1993) did reach south of -47° , yielding 39 objects). In addition, Lepine's continuing SUPERBLINK survey will provide a vast database of proper-motion systems down to 0'.'015 yr⁻¹. He has already published the northern portion of the survey, which yielded 61,977 objects (Lépine & Shara 2005).

Our goal since the beginning of the SCR search has been to complete a comprehensive proper-motion survey of the neglected southern sky. Adding results from this paper, we have searched the sky from the south celestial pole to declination -47° for objects with 10″.00 yr⁻¹ $\geq \mu \geq 0$ ″.18 yr⁻¹, where the lower cutoff has been chosen to match the NLTT.

¹VizieR Online Data Catalogue, I/98A (Luvten 1995)

2. SEARCH CRITERIA

This phase of the SCR search uses techniques identical to our earlier efforts, simply with a lower proper motion cutoff. Identical methodology allows us to assess completeness comprehensively and compare statistics from the various search phases. The search techniques are described in detail in Paper VIII in this series (Hambly et al. 2004). Additional phases of the search can be found in Papers X (Henry et al. 2004), XII (Subasavage et al. 2005a), and XV (Subasavage et al. 2005b). Briefly, the SCR search utilizes four of the Schmidt survey photographic plates available in each ESO/SRC survey field, which provide astrometric and photometric information in the B_J , ESO-R, R_{59F} and I_{IVN} photographic passbands. Two distinct epochs in the R band come from the ESO (first epoch; also known as ESO-R) and UK (second epoch; also known as AAO-R) Schmidt telescope surveys. Sources must be detected on at least three plates, and are required to have R_{59F} brighter than magnitude 16.5.

We introduce clear nomenclature here in an effort to sort three categories of systems revealed during the SCR proper motion search. MOTION systems have $\mu \geq 1''.00 \text{ yr}^{-1}$ (Paper VIII). The 1''.00 yr⁻¹ cutoff is convenient, and has been studied in detail by (Jao 2004). SLOWMO systems have 1''.00 yr⁻¹ > $\mu \geq 0''.50 \text{ yr}^{-1}$ (Papers XII and XV). The 0''.50 yr⁻¹ cutoff has been selected to match the famous Luyten Half Second (LHS) sample. MINIMO systems have 0''.50 yr⁻¹ > $\mu \geq 0''.18 \text{ yr}^{-1}$, where the lower cutoff is designed to match that of the NLTT catalogue. Papers XII and XV include some MINIMO stars because we pushed to $\mu = 0''.40 \text{ yr}^{-1}$ to ensure that we picked up any "LHS equivalent" systems with $\mu \sim 0''.50 \text{ yr}^{-1}$. Those papers also split the southern sky into two portions: Paper XII covered the sky from declinations -90° to -47° , while Paper XV stretched north to the celestial equator. In this paper, we match the boundaries of the search in Paper XII and report the remainder of the MINIMO systems in the range 0''.40 yr⁻¹ > $\mu \geq 0''.18 \text{ yr}^{-1}$.

Photographic plates scanned and folded into the SuperCOSMOS database are $6^{\circ} \times 6^{\circ}$ with a 0.5° overlap of adjacent fields on each side, providing ~ 25 square degrees of unique sky coverage for each field. Two hundred fields have been included in the present search, yielding a total coverage of ~ 5000 square degrees, corresponding to 12% of the entire sky. In this region a total of 7410 candidate objects were detected, more than four times the amount of candidates found in Paper XII. Fields shown as whitespaces in Figure 1 were omitted because of crowding near the Magellanic Clouds or Galactic Plane, or because those plate regions had epoch spreads inadequate for reliable proper motion measurements. It is worth noting that three more plates have been omitted in this paper than in Paper XII because longer plate epoch separations are required to reliably determine slower proper motions. The total region omitted amounts to 2.4% of the entire sky.

After object detection and parameterization (see Hambly et al. (2001b)), coordinates are given to each detection making use of a grid of reference stars with known coordinates distributed over the plates as described in Hambly et al. (2001a). The default SuperCOSMOS Sky Survey (SSS) pairing is then used to extract proper motion objects (a full description can be found in (Hambly et al. 2001a)). The pairing is set to exclude all images that appear on all four plates having an astrometric solution that indicates a proper motion less than the cut off for this search at 0'.18 yr⁻¹ and a goodness-of-fit parameter of $\chi^2 < 1.0$ (Hambly et al. 2004). Each image either not paired or having inconsistent astrometric solutions due to incorrect pairing are then processed one at a time using every possible combination to find a pair out to the upper limit of the SCR search, 0'.40 yr⁻¹ for this portion of the search. Proper motions so determined are relative to the mean reference frame defined for all stars on the plates, because all stars are used to map out small scale systematic errors in positions due to the photographic and measurement processes (see for example (Hambly et al. 2001a)).

We continue to use a three-stage sifting method discussed in detail in Paper XII to remove false detections. Generally, if a candidate object survives two color checks and a check of the ellipticity quality flag, it advances to a check of databases for previous identifications. Coordinates of these objects are cross-checked using both VizieR and SIMBAD to identify previously known objects. In VizieR, a ten arcminute radius is used to match SCR detections with both the NLTT and The Liverpool-Edinburgh High Proper Motion (LEHPM) catalogues. If the coordinates of an SCR object are within a few arcminutes of a catalogue object, and the proper motion and magnitude match, then the target object is labeled as previously known. As a final discovery verification, all potentially new objects are checked against SIMBAD to determine if they have been previously reported as proper motion objects. One class of known objects, GSC objects from the Hubble Space Telescope (HST) Guide Star Catalogue, is not considered previously "found", as those stars have merely been selected as pointing reference points for HST, not as scientifically noteworthy sources. Some near matches were found to be common proper motion (CPM) companions to previously known proper motion objects. All of these new companions are visually inspected for accuracy and are discussed in §5.3.

If the object is not found to be previously known, a visual inspection is done to confirm its veracity. Visual inspections are carried out by blinking the B_J and R_{59F} SuperCOSMOS digitally scanned plate images, which have a sufficient spread in epochs to confirm or refute derived proper motions. Thus, all objects reported here have been confirmed by eye, but some small number of real objects may have been discarded because visual inspections were not carried out for sources that did not pass the three checks.

In keeping with previous discovery statistics, we compare the successful hit rates (real

proper motion objects / total candidates extracted) for the MOTION, SLOWMO, and MIN-IMO samples in the portion of the sky covered by all three, from declinations -90° to -47° (not including individual plate regions that were discarded in any search). The hit rates are 6.6% for MOTION systems, 78.6% for SLOWMO systems, and 78.1% for MINIMO systems. These hit rates take into account new, known, duplicate, and "garbage" (not real) objects. In Figure 2, we show a plot of proper motion vs. percent successful hit rate for the entire SCR sample having $\mu \geq 0''.18 \text{ yr}^{-1}$ south of declination -47° . The SCR search has a sweet spot near $\mu \sim 0''.45 \text{ yr}^{-1}$, where the success rate in picking up proper motion objects is 93%. This high success rate deteriorates toward faster and slower proper motion regimes, where the SCR search is more susceptible to false detections. Causes include mistaken object movement from one plate to another when there are slight shifts between the plates, focus abnormalities, spurious objects created via plate defects, and bright star halos. In Table 1, SCR objects in the various papers have been categorized into the MOTION, SLOWMO, and MINIMO samples and discovery statistics are shown for the entire SCR sample.

3. COMPARISON TO PREVIOUS PROPER-MOTION SURVEYS

The NLTT catalogue lists 58693 objects with $\mu \geq 0$. 18 yr⁻¹. Of these, 2278 objects meet the search criteria of this paper and have estimated red magnitudes of 16.5 or brighter. We recover 1852 of 2278 objects found in the fields we searched, resulting in an 81% recovery rate. Several factors contribute to the 19% of unrecovered stars. Our proper motions are accurate to ~ 0.000 yr⁻¹ and our magnitudes to ~ 0.3 mag. Proper motions and magnitudes in the NLTT in some cases differ from ours, which causes us to drop some objects that were included in the NLTT. On rare occasions we also miss stars that are lost on recent plates due to mergers, but were uncorrupted during previous efforts. Our SCR search has trouble picking up brighter sources because of halo effects present on the photographic plates. The brightest NLTT source we identified in the search is at $R_{59F} \sim 5.4$ mag while the brightest NLTT source in this portion of the sky is R ~ 1.6 mag. Here we compare the results from our SCR survey to date for declinations -90° to -47° to the proper motion surveys listed in Table 2° . The numbers listed reflect only the total number of entries in each work — we have not confirmed that all sources by other groups are both real and original.

 $^{^2}$ For samples that were reported in 1950 coordinates, we have not computed 2000 coordinates or slid stars because of proper motion over 50 years. The number of objects that may have slipped out of the sample by moving north of -47° is expected to be small, and a comparable number of replacement objects likely have slipped south.

4. DATA

Rather than list all of the 1606 new MINIMO systems reported in this paper explicitly, we give the first five lines in Table 3; the full Table can be found in the electronic version of this paper. In Table 4 we highlight the 31 systems for which we estimate distances of less than 25 pc, and 13 additional white dwarf candidates. As in previous SCR search papers, in Table 3 and 4 we list SCR names, coordinates, relative proper motions, plate magnitudes from SuperCOSMOS, infrared photometry from 2MASS, the $R_{59F} - J$ color, a distance estimate, and notes.

All coordinates are for epoch and equinox J2000.0 and are computed using the Two Micron All Sky Survey (2MASS) coordinates and adjusted to epoch 2000.0 using the SCR proper motions and position angles. From our search algorithm, the average proper motion errors are \sim 0".010 yr⁻¹. We show in Figure 3 that our proper motion and position angle measurements are consistent with those in NLTT and Hipparcos by examining 298 MINIMO stars which had data in both catalogues.³ The results indicate that the SCR proper motions and position angles have an average deviation of \sim 0".025 yr⁻¹ and \sim 6.8° compared to NLTT motions and \sim 0".020 yr⁻¹ and \sim 3.9° compared to Hipparcos. We also show that the NLTT and Hipparcos proper motions and position angles show average deviations in proper motions of \sim 0".019 yr⁻¹ and \sim 5.1° when compared to each other. Comparison of the three outlying data points in position angle in the SCR vs. NLTT and Hipparcos vs. NLTT plots indicates that these NLTT measurements are incorrect. The consistency between SCR and Hipparcos is particularly encouraging because Hipparcos only observed stars brighter than $V \sim 12$, and these are the stars with the poorest measured proper motions in the SCR survey.

Photographic magnitudes are given in Table 3 and 4 for three plate emulsions: B_J , R_{59F} , and I_{IVN} . Plate magnitude errors are typically less than 0.3 mag for sources fainter than 15th mag, with errors increasing for brighter objects because of systematic errors (Hambly et al. 2001b). Plate color errors are typically only 0.07 mag. 2MASS JHK_s photometry and a representative color, $R_{59F} - J$, generated using two of the most reliable photometric measurements, are given. All JHK_s infrared photometry is extracted from 2MASS via VizieR and these magnitudes were spot-checked by eye for accuracy. 2MASS magnitude errors are 0.03 mag or less in most cases. This holds true unless J > 15, H > 14.5 or $K_s > 14$, for which the errors are typically 0.05 mag or greater.

The six-band photometry is used to generate 12 colors that are utilized to compute

 $^{^3}$ NLTT proper motion data are quantized south of DEC -45° because those proper motions are reported to hundredths, whereas north of DEC -45° proper motions are reported to thousandths.

distance estimates, as described in Hambly et al. (2004). All estimates assume that the objects are single, main sequence stars. The scatter is 26%, defined as the mean of the absolute values of the differences between distances for stars with trigonometric parallaxes and distances estimated via the relations. In cases where objects are too blue for the relations, no distance is listed. In a few cases the B_J and/or I_{IVN} plate magnitudes are not determined (likely causes include confusing sources and plate defects), making the distance estimate less reliable. Thirteen white dwarf and 174 subdwarf candidates have erroneous distances (listed in brackets) from the suite of relations because they are not main sequence stars; more accurate estimates are given in the notes for the white dwarfs. Overall, we find two systems within 10 pc, 29 between 10 and 25 pc, and 377 between 25 and 50 pc.

Some of the CPM candidates were not revealed during the SCR search because of confusion with another source, or because the companion was fainter than our magnitude cutoff; these were however, noticed during the blinking process. In these cases the objects are investigated using SIMBAD and VizieR to check for previous identifications. If the object was not previously known, we use SuperCOSMOS and 2MASS magnitudes to obtain the six colors used to compute distance estimates, and proper motion data from SuperCOSMOS to compute proper motions and position angles.

5. ANALYSIS

5.1. Color-Magnitude Diagram

Plotted in Figure 4 is a color magnitude diagram comparing the new SCR objects (open circles) to the known objects (small points) from this phase of the search. Data points below $R_{59F} = 16.5$ are CPM companions noticed durring the blinking process. As in Papers XII and XV, the bulk of the new discoveries are fainter and redder than the known stars, including three objects, SCR 0838-5855, SCR 1826-6542, and SCR 2241-6119B with $R_{59F} - J > 5.5$. Unlike the sources extracted in our previous efforts, there are more new discoveries featured in this paper that are brighter and bluer than in previous discoveries. In fact, there are 9 new discoveries with R_{59F} brighter than 10th magnitude that had not been identified previously. The point at $R_{59F} = 8.14$ is SCR 1914-7109, which is too blue for us to estimate a distance using the plate-2MASS relations.

As in comparable plots in previous papers, several white dwarf candidates are clearly separated from the bulk of the sample. The subdwarf population is less well-defined, but a population of subdwarfs can be detected below the concentration of main sequence stars.

5.2. Reduced Proper Motion Diagram

Shown in Figure 5 is the reduced proper motion (RPM) diagram for objects found in this search, similar to the RPM diagrams shown in Papers XII and XV. The RPM diagram relies on the statistical (inverse) relationship between proper motion and distance: objects that have larger distances generally have smaller proper motions. As such, it can be used to separate white dwarfs and (less clearly) subdwarfs from main-sequence stars. While this assumption is not always valid, it is a fairly reliable indicator of luminosity class for most stars. As in previous papers, the relation used to determine H_R is

$$H_R = R_{59F} + 5 + 5 \log \mu.$$

A comparison of Figures 4 and 5 shows that the RPM diagram is slightly better at separating the three samples.

There is a clear break separating the white dwarfs from the rest of the sample. The arbitrary dashed line between the subdwarfs and white dwarfs is the same as used in Paper XV, although the proper motions are smaller. In this region of the diagram, we find 12 new white dwarf candidates: SCR 0004-6120B, SCR 0018-6851, SCR 0104-5742B, SCR 0150-7207, SCR 0245-6038, SCR 0355-5611, SCR 0840-7826, SCR 0857-6032, SCR 1821-5951, SCR 2020-7806, SCR 2032-4948B, and SCR 2354-6023. One additional candidate, SCR 0429-5423B, was noticed while blinking to have the colors consistent with a white dwarf, but lacks the 2MASS data to plot in the RPM diagram, bringing the total number of white dwarf candidates for this paper to 13. One object SCR 1800-5112B is a close double with blended photometry in SuperCOSMOS, which puts it inside the white dwarf regime of the RPM diagram. The infrared colors however are not consistent with a white dwarf, and therefore is not considered a white dwarf candidate. Of the 13 candidates, three (SCR 0104-5742B, SCR 0150-7207 and SCR 1821-5951) have been spectroscopically confirmed (results to be presented in a future publication). Each is listed in Table 4 with a bracketed erroneous distance estimate assuming the object is a main sequence star. We include a distance estimate based on the assumption of the source being a main sequence member because large distances can be used to flag possible white dwarfs. All white dwarfs are estimated to be beyond 700 pc except SCR 0018-6851, SCR 0150-7207, SCR 0429-5423B, SCR 0857-6032, and SCR 1821-5951 which have blended SuperCOSMOS photometry, no 2MASS data, or are too blue for the relations. In the notes we give more accurate distance estimates assuming the objects are single white dwarfs and using the relation of (Oppenheimer et al. 2001), with adopted errors of 20% as given by the authors. This brings the total number of white dwarf candidates to 23 for the SCR survey.

To be consistent with Paper XV, subdwarf candidates are selected to have $R_{59F}-J>1.0$ and $H_R>4.0$ mag above the dashed line separating the white dwarfs from the subdwarfs. As with the white dwarf cutoff line, the subdwarf cutoff used is arbitrary, yet provides a fairly accurate distinction between the subdwarfs and main sequence classes. Although some contamination of the sample is expected, we count a total of 174 new subdwarf candidates from this paper. This brings the total number of SCR subdwarf candidates to date to 238.

5.3. New Common Proper Motion Systems

In this search we find a total of 54 new likely CPM systems, including 52 doubles and two triples (i.e. 56 companions). All primaries, companions and their proper motions are recorded in Table 5, the separations and position angles are of companions relative to the primary star. Distance estimates for multiple components that agree to within a factor of two are considered to be consistent, given the errors of the distance estimating relations. Twenty-two pairs of objects were discovered via the automated search and were subsequently noticed to have common proper motion. Twenty-five additional new SCR companions not revealed during the automated search were noticed during the blinking process. Nine previously known objects were noticed by eye to have common proper motions to SCR stars discovered during the automated search.

In Figures 6 and 7, we compare the proper motions and position angles for the 52 pairs having complete sets of μ and θ (because of blending in four systems, SuperCOSMOS data could not be obtained for the potential companion, and they were too close to obtain accurate manual measurements). Values obtained through the systematic SCR trawl are shown with filled circles, while open circles are used if a companion was noticed during the blinking process of the SuperCOSMOS scans. Data were then retrieved manually from SuperCOSMOS for the noticed companions. Usually, such companions are fainter than our search cutoff of $R_{59F} = 16.5$.

As is typical with proper motion surveys, the position angles of the proper motions are better determined than the proper motions themselves, which are especially volatile at these relatively low values. Hence, the position angles are given greater weight when deciding whether or not two sources really are part of the same system. The average scatter for the proper motions and position angles are $\sim 0.020 \, \mathrm{yr^{-1}}$ and $\sim 5.0 \, \mathrm{degrees}$, respectively, which is consistent with comparisons of SCR data to NLTT and Hipparcos, as discussed previously.

5.4. Comments on Individual Systems

SCR 0838-5855 has $R_{59F} = 16.11$ and $R_{59F} - J = 5.80$. This is likely to be a late M dwarf at an estimated distance of only 8.4 pc. This is a high priority target on our CTIOPI parallax program at the CTIO 0.9m (Jao et al. 2005; Henry et al. 2006).

SCR 0927-6239BC are common proper motion companions to NLTT 21827. The B component has a separation of 200″.9 at position angle 92.0° from the primary. The C component is not in 2MASS and has a separation of 316″.2 at a position angle of 59.6° from the primary. See Table 5.

SCR1441-7338 has $R_{59F} = 16.14$ and $R_{59F} - J = 4.95$ with a distance estimate of 19.0 pc.

SCR 1826-6542 has $R_{59F} = 16.43$ and $R_{59F} - J = 5.86$. This is likely to be a late M dwarf at an estimated distance of only 9.2 pc.

SCR 1914-7109 is very bright, with $R_{59F} = 8.14$ and $R_{59F} - J = -0.54$. It is too blue for us to estimate a distance using the plate-2MASS relations.

SCR 2057-6358ABC is a possible triple system with the A and B component separated by less than 2″.00, which have blended SuperCOSMOS photometry, but separated in 2MASS. Both the B and C components were noticed by eye during the blinking process. The C component has a separation of 261″.5 at position angle 121.6° from the primary. See Table 5.

6. DISCUSSION

Including all papers pertaining to the SCR proper motion survey, we have discovered 1967 new systems (2030 objects) with $\mu \geq 0''.18 \text{ yr}^{-1}$ between declinations -90° and 0° . Systems reported in previous papers are represented by filled circles in the sky map of SCR systems in Figure 8; systems in this paper are represented by open circles.

The 1606 systems in this paper comprise 82% of the entire SCR sample and bring the total number south of -47° to 1761 systems (1817 objects). From this paper, there are 13 likely white dwarfs and 174 subdwarf candidates. Three of the white dwarfs, (but none of the subdwarfs) have been spectroscopically confirmed, while the rest remain to be targeted in future spectroscopic efforts to confirm their luminosity classes.

Discovery statistics for the entire SCR sample, separated by distance horizons, are given in Table 6. In order to be consistent with previous SCR papers, new common proper motion

candidates that are companions to known objects and probable white dwarfs (because their distance estimates require a different set of relations) are not included. For all proper motion bins except the last, we have searched the entire southern sky; for the last bin only -47° to -90° has been searched. In the complete sample of new SCR systems to date, 7 are estimated to be within 10 pc, and 67 additional systems lie between 10 and 25 pc. Of the 1606 systems reported in this paper, two were estimated to be within 10 pc, with an additional 29 between 10 and 25 pc. This illustrates that even in this relatively slow proper motion regime there are nearby stars hidden in the solar neighborhood. Should they prove to be within 10 pc, the two nearest stars reported in this paper would rank as the 10th (0″.311 yr⁻¹ SCR 1826-6542) and 11th (0″.320 yr⁻¹ for SCR 0838-5855) slowest systems in the RECONS sample of 248 systems within 10 pc (Henry et al. 2006).

Although the counts of new 10 pc candidates are small in each proper motion bin, the largest number of candidates between 10 and 25 pc is found in the slowest proper motion bin, even though only a portion of the southern sky has been searched. We anticipate that continuing searches for MINIMO systems in the southern sky will be a promising endeavor for finding additional nearby stars.

7. ACKNOWLEDGMENTS

Funding for the SuperCOSMOS Sky Survey was provided by the UK Particle Physics and Astronomy Research Council. N.C.H. would like to thank colleagues in the Wide Field Astronomy Unit at Edinburgh for their work in making the SSS possible; particular thanks go to Mike Read, Sue Tritton, and Harvey MacGillivray. The RECONS team at Georgia State University wishes to thank NASA's *Space Interferometry Mission* and the National Science Foundation (grant AST 05-07711) for their continued support of our solar neighborhood exploration. This work has made use of the SIMBAD, VizieR, and Aladin databases operated at the CDS in Strasbourg, France. We have also used data products from the Two Micron All Sky Survey, which is a joint project of the University of Massachusetts and the Infrared Processing and Analysis Center, funded by NASA and NSF.

REFERENCES

Deacon, N. R., Hambly, N. C., & Cooke, J. A. 2005, A&A, 435, 363

Giclas, H. L., Burnham, R., & Thomas, N. G. 1971, Flagstaff, Arizona: Lowell Observatory, 1971

- Giclas, H. L., Burnham, R., & Thomas, N. G. 1978, Lowell Observatory Bulletin, 8, 89
- Hambly, N. C., Henry, T. J., Subasavage, J. P., Brown, M. A., & Jao, W. 2004, AJ, 128, 437
- Hambly, N. C., Davenhall, A. C., Irwin, M. J., & MacGillivray, H. T. 2001c, MNRAS, 326, 1315
- Hambly, N. C., Irwin, M. J., & MacGillivray, H. T. 2001, MNRAS, 326, 1295
- Henry, T. J., Jao, W.-C., Subasavage, J. P., Beaulieu, T. D., Ianna, P. A., Costa, E., & Méndez, R. A. 2006, AJ, 132, 2360
- Henry, T. J., Subasavage, J. P., Brown, M. A., Beaulieu, T. D., Jao, W.-C., & Hambly, N. C. 2004, AJ, 128, 2460
- Jao, W.-C. 2004, Ph.D. Thesis
- Jao, W.-C., Henry, T. J., Subasavage, J. P., Brown, M. A., Ianna, P. A., Bartlett, J. L., Costa, E., & Méndez, R. A. 2005, AJ, 129, 1954
- Lépine, S., & Shara, M. M. 2005, AJ, 129, 1483
- Lépine, S. 2005, AJ, 130, 1247
- Luyten, W. J. 1979, LHS Catalogue (Minneapolis: Univ. of Minnesota Press)
- Luyten, W. J. 1980, Proper Motion Survey with the 48-inch Telescope, Univ. Minnesota, 55, 1 (1980), 55, 1
- Luyten, W. J. 1995, VizieR Online Data Catalog, 1098, 0
- Oppenheimer, B. R., Hambly, N. C., Digby, A. P., Hodgkin, S. T., & Saumon, D. 2001, Science, 292, 698
- Pokorny, R. S., Jones, H. R. A., & Hambly, N. C. 2003, A&A, 397, 575
- Pokorny, R. S., Jones, H. R. A., Hambly, N. C., & Pinfield, D. J. 2004, A&A, 421, 763
- Ruiz, M. T., Takamiya, M. Y., Mendez, R., Maza, J., & Wishnjewsky, M. 1993, AJ, 106, 2575
- Ruiz, M. T., Wischnjewsky, M., Rojo, P. M., & Gonzalez, L. E. 2001, ApJS, 133, 119
- Scholz, R.-D., Irwin, M., Ibata, R., Jahreiß, H., & Malkov, O. Y. 2000, A&A, 353, 958

Scholz, R.-D., Szokoly, G. P., Andersen, M., Ibata, R., & Irwin, M. J. 2002, ApJ, 565, 539

Subasavage, J. P., Henry, T. J., Hambly, N. C., Brown, M. A., & Jao, W. C. 2005, AJ, 129, 413

Subasavage, J. P., Henry, T. J., Hambly, N. C., Brown, M. A., Jao, W. C., & Finch, C. T. 2005, AJ, 130, 1658

Wroblewski, H., & Costa, E. 1999, A&AS, 139, 25

Wroblewski, H., & Costa, E. 2001, A&A, 367, 725

Wroblewski, H., & Torres, C. 1989, A&AS, 78, 231

Wroblewski, H., & Torres, C. 1991, A&AS, 91, 129

Wroblewski, H., & Torres, C. 1994, A&AS, 105, 179

Wroblewski, H., & Torres, C. 1996, A&AS, 115, 481

Wroblewski, H., & Torres, C. 1997, A&AS, 122, 447

This preprint was prepared with the AAS LATEX macros v5.2.

Table 1. Discovery Statistics for Entire SCR Sample $^{\rm a}$

	MOTION ^b	SLOWMOc	MINIMOd
New Discoveries	9	142	1879
Knowns	171	1159	5581
Duplicates	15	91	864
Garbage	1989	344	3613
Total Hits	2184	1736	11937

 $^{^{\}rm a}{\rm Entire}$ SCR Sample, including all previous SCR proper motion papers

 $^{^{\}rm b}{\rm MOTION}$ sample includes $\mu \geq 1\rlap.{''}00~{\rm yr}^{-1}$

 $^{^{\}rm c}{\rm SLOWMO~sample~includes~1.\!''00~yr^{-1}}>\mu\geq0.\!''50~{\rm yr^{-1}}$

 $^{^{\}rm d} \rm MINIMO~ sample~includes~ 0.\!^{\prime\prime}50~ \rm yr^{-1} > \mu \geq 0.\!^{\prime\prime}18~ \rm yr^{-1}$

Table 2. Number of NLTT Objects Discovered South of Declination $-47^{\circ a}$

Survey	$\mu \ge 1.00 \text{ yr}^{-1}$	$1''00 \text{ yr}^{-1} > \mu \ge 0''50 \text{ yr}^{-1}$	$0.50 \text{ yr}^{-1} > \mu \ge 0.18 \text{ yr}^{-1}$	Total	# of Publications	References ^b
NLTT	56	261	3529	3846	1	1
SuperCOSMOS-RECONS	5	70	1742	1817	5	2, 3, 4, 5, 6
Wroblewski and collaborators	3	28	488	519	4	7, 8, 9
SUPERBLINK	1	43	29	73	1	10
Scholz and collaborators	2	11	55	68	2	11, 12
Ruiz and collaborators	0	2	37	39	1	13
SIPS	7	20	0	27	1	14
Oppenheimer et al.	1	4	2	7	1	15
Pokorny et al.	mixed	mixed	mixed	mixed	2	16, 17

^aNumbers listed indicate objects reported as "new" in the survey publications. Pokorny did not differentiate between new and previously known objects, so the entry is labled as mixed.

^bReferences include (1) Luyten (1979, 1980), (2,3,4,5,6) Hambly et al. (2004); Henry et al. (2004); Subasavage et al. (2005a,b), this paper, (7,8,9) Wroblewski & Torres (1989, 1991, 1994), (10) Lépine (2005), (11,12) Scholz et al. (2000, 2002), (13) Ruiz et al. (1993), (14) Deacon et al. (2005), (15) Oppenheimer et al. (2001), (16,17) Pokorny et al. (2003, 2004)

Table 3. Characteristics of New SCR Systems with 0″.40 yr^-1 > $\mu \ge$ 0″.18 yr^-1 from $-90^{\circ} < \delta \le -47^{\circ}$

Name	RA (J2000)	DEC (J2000)	$\mu \ ('')$	θ (°)	B_J	R_{59F}	I_{IVN}	J	Н	K_s	$R_{59F} - J$	Est Dist (pc)	Notes
SCR 0001-7015	00 01 56.59	-70 15 08.4	0.202	141.1	18.22	16.20	14.64	13.36	12.79	12.66	2.84	142.5	
SCR 0003-6021	00 03 59.01	-60 21 58.1	0.249	145.1	17.84	15.68	12.92	11.68	11.08	10.75	4.00	35.3	
SCR 0004-5740	$00\ 04\ 26.79$	-57 40 02.7	0.181	091.2	16.00	13.87	12.36	11.47	10.87	10.65	2.41	66.0	
SCR 0004-6120A SCR 0004-6120B	00 04 56.20 00 04 45.41	-61 20 58.0 -61 23 40.0	$0.180 \\ 0.171$	129.0 127.6	13.63 16.87	11.28 16.76	9.94 16.54	$9.66 \\ 16.44$	9.08 15.94	$8.81 \\ 16.48$	1.62 0.33	35.8 [1216.2]	а а , b , с

^aCommon proper motion companion; see Table 5

^bWhite dwarf candidate picked from RPM diagram, plate distance [in bracket] is incorrect; see Table 4

^cNot detected during automated search but noticed by eye during the blinking process

^dSubdwarf candidate picked from RPM diagram; plate distance [in bracket] is incorrect

 $^{^{\}mathrm{e}}$ Source not in 2MASS

Table 4. Characteristics of New SCR Systems Estimated to be Nearer than 25 Parsecs and New White Dwarf Candidates with 0'.40 yr⁻¹ > $\mu \ge$ 0'.18 yr⁻¹ from $-90^{\circ} < \delta \le -47^{\circ}$

Name	RA (J2000)	DEC (J2000)	$\mu \ ('')$	$^{ heta}_{(^{\circ})}$	B_J	R_{59F}	I_{IVN}	J	Н	K_s	$R_{59F} - J$	Est Dist (pc)	Notes
				SCR Re	d Dwarf	candidat	tes < 25p	ос					
SCR 0100-7904	01 00 56.08	-79 04 25.2	0.379	215.3	13.69	11.69	9.98	8.79	8.16	7.88	2.89	14.9	
SCR 0135-6127	01 35 53.66	-61 27 11.1	0.255	256.8	15.61	13.67	11.80	10.05	9.53	9.24	3.61	20.8	
SCR 0138-5353	01 38 20.51	-53 53 26.1	0.297	071.0	15.70	13.69	11.73	10.27	9.69	9.42	3.42	24.2	
SCR 0211-6108	02 11 35.42	-61 08 53.8	0.234	060.8	11.68	9.73	9.23	8.67	8.15	8.07	1.06	22.9	
SCR 0232-8458	02 32 50.12	-84 58 09.5	0.220	141.9	12.31	10.17	9.87	8.99	8.34	8.18	1.17	24.9	
SCR 0246-7024	$02\ 46\ 02.25$	-70 24 06.3	0.259	113.2	15.71	13.32	10.71	9.83	9.32	9.01	3.49	20.0	
SCR 0527-7231	$05\ 27\ 06.99$	-72 31 20.0	0.368	018.3	16.01	13.96	11.76	10.33	9.76	9.47	3.63	22.6	
SCR 0635-6722	06 35 48.81	-67 22 58.5	0.383	340.0	12.21	9.83	8.66	8.54	7.95	7.69	1.29	22.7	
SCR 0838-5855	08 38 02.24	-58 55 58.7	0.320	188.9	18.44	16.11	12.43	10.30	9.70	9.26	5.80	8.4	
SCR 1147-5504	11 47 52.49	-55 04 11.9	0.192	011.3	14.95	12.23	10.25	9.67	9.08	8.81	2.56	24.1	
SCR 1217-7810	12 17 26.93	-78 10 45.9	0.212	056.6	17.54	15.69	13.14	11.19	10.64	10.35	4.49	24.5	
SCR 1220-8302	12 20 03.71	-83 02 29.2	0.243	244.2	17.03	14.93	12.79	10.97	10.39	10.07	3.96	25.0	
SCR 1224-5339	12 24 24.44	-53 39 08.8	0.189	251.9	16.93	14.77	12.30	10.50	9.93	9.64	4.26	18.1	
SCR 1347-7610	13 47 56.80	-76 10 20.0	0.194	089.7	12.39	10.26	8.88	8.62	8.01	7.77	1.64	22.5	
SCR 1420-7516	14 20 36.84	-75 16 5.9	0.195	243.7	14.22	12.68	10.44	9.44	8.90	8.63	3.23	21.3	
SCR 1441-7338	$14\ 41\ 14.42$	-73 38 41.4	0.207	029.0	18.27	16.14	13.04	11.19	10.60	10.26	4.95	19.0	
SCR 1448-5735	14 48 39.82	-57 35 17.7	0.202	188.8	12.47	10.59	12.46	9.14	8.55	8.43	1.45	18.2	
SCR 1456-7239	14 56 02.29	-72 39 41.4	0.207	225.0	16.50	14.22	11.99	10.62	10.05	9.74	3.60	24.9	
SCR 1738-5942	17 38 41.02	-59 42 24.4	0.280	148.2	16.57	14.20	11.92	10.38	9.83	9.58	3.82	20.8	
SCR 1820-6225	18 20 49.35	-62 25 52.7	0.190	164.8	13.35	11.17	8.43	9.13	8.48	8.29	2.04	22.4	
SCR 1826-6542	18 26 46.83	-65 42 39.9	0.311	178.9	18.68	16.43	12.91	10.56	9.96	9.54	5.86	9.2	
SCR 1853-7537	$18\ 53\ 26.61$	-75 37 39.8	0.304	168.7	12.20	9.85	9.09	8.34	7.73	7.49	1.51	20.0	
SCR 1856-4704	18 56 38.40	-47 04 58.3	0.252	131.3	16.29	13.92	11.64	10.29	9.74	9.44	3.63	21.4	
SCR 1926-8216	19 26 48.64	-82 16 47.6	0.195	172.5	12.22	10.00	10.20	9.04	8.42	8.30	0.96	17.3	
SCR 1932-5005	$19\ 32\ 48.64$	-50 05 38.9	0.257	157.5	16.86	14.50	11.99	10.75	10.11	9.84	3.75	24.4	
SCR 1959-6236	19 59 33.55	-62 36 13.4	0.189	288.7	17.47	15.35	12.67	11.06	10.49	10.22	4.29	24.3	
SCR 2016-7531	$20\ 16\ 11.25$	-75 31 04.5	0.253	081.3	17.06	14.74	12.24	10.46	9.86	9.50	4.28	16.2	
SCR 2042-5737	$20\ 42\ 46.44$	-57 37 15.3	0.264	142.6	15.06	13.22	11.55	9.97	9.52	9.03	3.25	22.7	
SCR 2230-5244	$22\ 30\ 27.95$	-52 44 29.1	0.369	125.7	19.01	16.34		11.84	11.23	10.91	4.49	24.6	
SCR 2241-6119A	$22\ 41\ 44.36$	-61 19 31.2	0.184	124.0	15.64	13.65	11.70	10.20	9.61	9.35	3.44	23.2	a

Table 4—Continued

Name	RA (J2000)	DEC (J2000)	$_{('')}^{\mu}$	heta (°)	B_J	R_{59F}	I_{IVN}	J	H	K_s	$R_{59F}-J$	Est Dist (pc)	Notes
SCR 2335-6433A	23 35 18.43	-64 33 42.4	0.196	103.1	11.79	9.97	9.01	8.63	8.02	7.86	1.33	24.5	a
						SCR W	D Candio	dates					
SCR 0004-6120B	00 04 45.41	-61 23 40.0	0.171	127.6	16.86	16.76	16.53	16.43	15.93	16.47	0.32	[1216.2]	$^{\rm a}$, $^{\rm b}$, $^{\rm c}$, 59.3 \pm 11.9pc
SCR 0018-6851	$00\ 18\ 08.56$	-68 51 19.4	0.220	091.6	16.55	16.46	16.48	16.62	16.13	17.18	-0.16		$^{\mathrm{c}}$, $^{\mathrm{e}}$, $52.2\pm10.4\mathrm{pc}$
SCR 0104-5742B	$01\ 04\ 12.14$	-57 42 48.6	0.239	091.1	16.19	15.89	15.78	15.67	15.56	15.75	0.22	[872.1]	$^{ m a}$, $^{ m c}$, $^{ m f}$, $34.5 \pm 6.9 { m pc}$
SCR 0150-7207	$01\ 50\ 38.49$	-72 07 16.8	0.334	223.9	16.18	15.71	15.24	15.65	15.64	15.42	0.06		$^{ m c}$, $^{ m e}$, $^{ m f}$, $28.0\pm5.6{ m pc}$
SCR 0245-6038	$02\ 45\ 27.77$	-60 38 58.2	0.196	049.6	17.15	16.36	16.07	15.83	15.47	15.66	0.52	[821.9]	$^{\rm c}$, 29.9 \pm 6.0pc
SCR 0355-5611	$03\ 55\ 31.89$	-56 11 28.2	0.279	029.1	17.36	16.46	16.11	16.05	15.53	15.44	0.41	[755.9]	$^{\mathrm{c}}$, 28.9 \pm 5.8pc
SCR 0429-5423B	$04\ 29\ 05.93$	-54 23 03.6	0.170	39.7	17.91	17.08	16.97						$^{\mathrm{a}}$, $^{\mathrm{b}}$, $^{\mathrm{c}}$, $^{\mathrm{d}}$, $40.5\pm8.1\mathrm{pc}$
SCR 0840-7826	$08\ 40\ 29.00$	-78 26 46.0	0.399	010.3	16.06	15.82	15.77	15.62	15.57	15.47	0.20	[763.9]	$^{\rm c}$, 34.8 \pm 7.0pc
SCR 0857-6032	$08\ 57\ 08.21$	-60 32 45.4	0.217	333.3	15.20	15.37	15.45	15.94	16.20	15.78	-0.56		$^{\mathrm{c}}$, $^{\mathrm{e}}$, $38.2\pm7.6\mathrm{pc}$
SCR 1821-5951	$18\ 21\ 59.54$	-59 51 48.5	0.365	194.9	17.49	16.31	15.72	15.20	15.00	14.90	1.11	[588.9]	$^{\mathrm{c}}$, $^{\mathrm{f}}$, 22.2 \pm 4.4pc
SCR 2020-7806	$20\ 20\ 52.98$	-78 06 18.7	0.276	209.2	16.03	16.09	16.11	15.92	15.59	15.68	0.16	[834.9]	$^{\rm c}$, 49.1 ± 9.8pc
SCR 2032-4948B	$20\ 32\ 41.74$	-49 48 57.2	0.270	182.4	17.15	16.77	16.73	16.62	15.87	15.88	0.14	[900.1]	$^{\rm a}$, $^{\rm b}$, $^{\rm c}$, $48.7 \pm 9.7 {\rm pc}$
SCR 2354-6023	$23\ 54\ 50.63$	-60 23 16.0	0.230	098.6	16.31	16.06	15.93	15.87	15.77	16.31	0.18	[1127.8]	$^{\rm c}$, 38.6 \pm 7.7pc

^aCommon proper motion; see Table 5

^bNot detected during automated search but noticed by eye during the blinking process

^cWD candidate with unreliable distance estimate [in brackets]; more reliable WD distance estimate in notes

 $^{^{\}rm d}$ Not in 2MASS

^eAll colors are too blue or too red for distance relations

^fWD confirmed via spectroscopy; results to be published in a future paper by co-author Subasavage

Table 5. Common Proper Motion Systems

("") (°) (pc) ("") (°) (pc) ("") (°) (pc) ("") (°) HD 120056	
HD 158866 0.235 188.4 (13.1) SCR 1746-8211B 0.228 184.9 14.5 76.5 290.8 c, Hipparcos distance NLTT 01733 0.250 115.3 36.1 SCR 0032-5528B 0.221 115.2 70.3 349.6 71.4 b NLTT 03566 0.257 87.5 27.9 SCR 0104-5742B 0.239 91.1 [872.1] 110.6 206.6 d, WD candidate at NLTT 13852 0.233 46.3 ··· SCR 0436-8233B 0.233 51.1 48.6 108.9 338.7 a, Hipparcos distance NLTT 15903 0.223 17.9 36.4 SCR 0551-8116B 0.233 19.5 56.5 99.6 266.1 NLTT 20147 0.222 342.8 (40.4) SCR 0843-5007B 0.225 338.8 74.1 24.0 64.3 b, c, Hipparcos distance NLTT 21827 0.231 312.1 53.9 SCR 0927-6239B 0.204 312.2 41.6 200.9 92.0 SCR 0927-6239C 0.197 309.0 ··· 316.2 59.6 b, e NLTT 26256 0.194 283.9 (12.5) SCR 1104-7856B 0.203 283.1 101.1 260.4 167.7 b, c, Hipparcos distance NLTT 36394 0.238 238.9 (36.9) SCR 1411-7525B 0.250 242.1 111.5 21.8 275.5 c NLTT 45592 0.174 178.9 (23.3) SCR 1755-7241B 0.199 175.2 60.3 102.2 273.7 b, c, Hipparcos distance NLTT 36394 0.238 238.9 (36.9) SCR 1755-7241B 0.199 175.2 60.3 102.2 273.7 b, c, Hipparcos distance NLTT 45592 0.174 178.9 (23.3) SCR 1755-7241B 0.199 175.2 60.3 102.2 273.7 b, c, Hipparcos distance NLTT 45592 0.174 178.9 (23.3) SCR 1755-7241B 0.199 175.2 60.3 102.2 273.7 b, c, Hipparcos distance NLTT 45592 0.174 178.9 (23.3) SCR 1755-7241B 0.199 175.2 60.3 102.2 273.7 b, c, Hipparcos distance NLTT 45592 0.174 178.9 (23.3) SCR 1755-7241B 0.199 175.2 60.3 102.2 273.7 b, c, Hipparcos distance NLTT 45592 0.174 178.9 (23.3) SCR 1755-7241B 0.199 175.2 60.3 102.2 273.7 b, c, Hipparcos distance NLTT 45592 0.174 178.9 (23.3) SCR 1755-7241B 0.199 175.2 60.3 102.2 273.7 b, c, Hipparcos distance NLTT 45592 0.174 178.9 (23.3) SCR 1755-7241B 0.199 175.2 60.3 102.2 273.7 b, c, Hipparcos distance NLTT 45592 0.174 178.9 (23.3) SCR 1755-7241B 0.199 175.2 60.3 102.2 273.7 b, c, Hipparcos distance NLTT 45592 0.174 178.9 (23.3) SCR 1755-7241B 0.199 175.2 60.3 102.2 273.7 b, c, Hipparcos distance NLTT 45592 0.174 178.9 (23.3) SCR 1755-7241B 0.199 175.2 60.3 102.2 273.7 b, c, Hipparcos distance NLTT 45592 0.174 178.9 (23.3) SCR 1755-7241	
NLTT 01733	ance at 100.70pc
NLTT 03566	e at 30.61pc
$\begin{array}{cccccccccccccccccccccccccccccccccccc$	
$\begin{array}{c ccccccccccccccccccccccccccccccccccc$	$34.5 \pm 6.9 \mathrm{pc}$
$\begin{array}{c ccccccccccccccccccccccccccccccccccc$	e at 46.46pc
NLTT 21827 0.231 312.1 53.9 SCR 0927-6239B 0.204 312.2 41.6 200.9 92.0 SCR 0927-6239C 0.197 309.0 \cdots 316.2 59.6 b , e NLTT 26256 0.194 283.9 (12.5) SCR 1104-7856B 0.203 283.1 101.1 260.4 167.7 b , c , Hipparcos distance NLTT 36394 0.238 238.9 (36.9) SCR 1411-7525B 0.250 242.1 111.5 21.8 275.5 c NLTT 45592 0.174 178.9 (23.3) SCR 1755-7241B 0.199 175.2 60.3 102.2 273.7 b , c , Hipparcos distance NLTT 45592 0.174 178.9 (23.3) SCR 1755-7241B 0.199 175.2 60.3 102.2 273.7 b , c , Hipparcos distance NLTT 45592 0.174 178.9 (23.3) SCR 1755-7241B 0.199 175.2 60.3 102.2 273.7 b , c , Hipparcos distance NLTT 45592 0.174 178.9 (23.3) SCR 1755-7241B 0.199 175.2 60.3 102.2 273.7 b , c , Hipparcos distance NLTT 45592 0.174 178.9 (23.3) SCR 1755-7241B 0.199 175.2 60.3 102.2 273.7 b , c , Hipparcos distance NLTT 45592 0.174 178.9 (23.3) SCR 1755-7241B 0.199 175.2 60.3 102.2 273.7 b , c , Hipparcos distance NLTT 45592 0.174 178.9 (23.3) SCR 1755-7241B 0.199 175.2 60.3 102.2 273.7 b , c , Hipparcos distance NLTT 45592 0.174 178.9 (23.3) SCR 1755-7241B 0.199 175.2 60.3 102.2 273.7 b , c , Hipparcos distance NLTT 45592 0.174 178.9 (23.3) SCR 1755-7241B 0.199 175.2 60.3 102.2 273.7 b , c , Hipparcos distance NLTT 45592 0.174 178.9 (23.3) SCR 1755-7241B 0.199 175.2 60.3 102.2 273.7 b , c , Hipparcos distance NLTT 45592 0.174 178.9 (23.3) SCR 1755-7241B 0.199 175.2 60.3 102.2 273.7 b , c , Hipparcos distance NLTT 45592 0.174 178.9 (23.3) SCR 1755-7241B 0.199 175.2 60.3 102.2 273.7 b , c , Hipparcos distance NLTT 45592 0.174 178.9 (23.3) SCR 1755-7241B 0.199 175.2 60.3 102.2 273.7 b , c , Hipparcos distance NLTT 45592 0.174 178.9 (23.3) SCR 1755-7241B 0.199 175.2 60.3 102.2 273.7 b , c , Hipparcos distance NLTT 45592 0.174 178.9 (23.3) SCR 1755-7241B 0.199 175.2 60.3 102.2 273.7 b , c , Hipparcos distance NLTT 45592 0.174 178.9 (23.3) SCR 1755-7241B 0.199 175.2 60.3 102.2 273.7 b , c , Hipparcos distance NLTT 45592 0.174 178.9 (23.3) SCR 1755-7241B 0.199 175.2 60.3 102.2 273.7 b , c , Hipparcos 1755 1755 1755 1755 1755 1755 1755 175	
$ \begin{array}{cccccccccccccccccccccccccccccccccccc$	ince at 93.63pc
NLTT 26256 0.194 283.9 (12.5) SCR 1104-7856B 0.203 283.1 101.1 260.4 167.7 b, c, Hipparcos distance NLTT 36394 0.238 238.9 (36.9) SCR 1411-7525B 0.250 242.1 111.5 21.8 275.5 c NLTT 45592 0.174 178.9 (23.3) SCR 1755-7241B 0.199 175.2 60.3 102.2 273.7 b, c, Hipparcos distance NLTT 45592 0.174 178.9 (23.3) SCR 1755-7241B 0.199 175.2 60.3 102.2 273.7 b, c, Hipparcos distance NLTT 45592 0.174 178.9 (23.3) SCR 1755-7241B 0.199 175.2 60.3 102.2 273.7 b, c, Hipparcos distance NLTT 45592 0.174 178.9 (23.3) SCR 1755-7241B 0.199 175.2 60.3 102.2 273.7 b, c, Hipparcos distance NLTT 45592 0.174 178.9 (23.3) SCR 1755-7241B 0.199 175.2 60.3 102.2 273.7 b, c, Hipparcos distance NLTT 45592 0.174 178.9 (23.3) SCR 1755-7241B 0.199 175.2 60.3 102.2 273.7 b, c, Hipparcos distance NLTT 45592 0.174 178.9 (23.3) SCR 1755-7241B 0.199 175.2 60.3 102.2 273.7 b, c, Hipparcos distance NLTT 45592 0.174 178.9 (23.3) SCR 1755-7241B 0.199 175.2 60.3 102.2 273.7 b, c, Hipparcos distance NLTT 45592 0.174 178.9 (23.3) SCR 1755-7241B 0.199 175.2 60.3 102.2 273.7 b, c, Hipparcos distance NLTT 45592 0.174 178.9 (23.3) SCR 1755-7241B 0.199 175.2 60.3 102.2 273.7 b, c, Hipparcos distance NLTT 45592 0.174 178.9 (23.3) SCR 1755-7241B 0.199 175.2 60.3 102.2 273.7 b, c, Hipparcos distance NLTT 45592 0.174 178.9 (23.3) SCR 1755-7241B 0.199 175.2 60.3 102.2 273.7 b, c, Hipparcos distance NLTT 45592 0.174 178.9 (23.3) SCR 1755-7241B 0.199 175.2 60.3 102.2 273.7 b, c, Hipparcos distance NLTT 45592 0.174 178.9 (23.3) SCR 1755-7241B 0.199 175.2 60.3 102.2 273.7 b, c, Hipparcos distance NLTT 45592 0.174 178.9 (23.3) SCR 1755-7241B 0.199 175.2 60.3 102.2 273.7 b, c, Hipparcos distance NLTT 45592 0.174 178.9 (23.3) SCR 1755-7241B 0.199 175.2 60.3 102.2 273.7 b, c, Hipparcos distance NLTT 45592 0.174 178.9 (23.3) SCR 1755-7241B 0.199 175.2 60.3 102.2 273.7 b, c, Hipparcos distance NLTT 45592 0.174 178.9 (23.2) SCR 1755-7241B 0.199 175.2 60.3 102.2 273.7 b, c, Hipparcos distance NLTT 45592 0.174 178.9 (23.2) SCR 1755-7241B 0.199 175.2 60.3 102.2 273.7 b, c, Hipparco	
NLTT 36394 0.238 238.9 (36.9) SCR 1411-7525B 0.250 242.1 111.5 21.8 275.5 $^{\circ}$ NLTT 45592 0.174 178.9 (23.3) SCR 1755-7241B 0.199 175.2 60.3 102.2 273.7 $^{\rm b}$, $^{\rm c}$, Hipparcos distance of the contraction of the c	
NLTT 45592 0.174 178.9 (23.3) SCR 1755-7241B 0.199 175.2 60.3 102.2 273.7 b, c, Hipparcos dista	ince at 47.46pc
	ince of 77.94pc
NLTT 49033 0.270 159.1 28.8 SCR 2019-4701B 0.265 158.1 52.5 67.9 86.9 ^b	
NLTT 49299 0.295 100.1 (22.9) SCR 2029-5757B 0.314 107.8 79.0 111.7 102.8 ^c , Hipparcos distance	e at 56.31pc
PPM 365916 0.259 135.1 (33.0) SCR 2237-6238B 0.191 127.4 69.6 118.8 107.6 ^c	
SCR 0004-6120A 0.180 129.0 35.8 SCR 0004-6120B 0.171 127.6 [1216.2] 179.6 205.5 ^b , ^d , WD candidate	at $59.3 \pm 11.9 pc$
SCR 0017-5036A 0.204 112.1 (83.6) NLTT 00918 \cdots \cdots \cdots \cdots a , b , c	
SCR 0025-5254A 0.196 101.2 44.4 SCR 0025-5254B 0.110 107.1 80.0 286.8 330.7 ^b	
SCR 0055-5529A 0.234 53.6 88.9 SCR 0055-5529B 0.212 52.6 \cdots 5.8 359.3 a , b	
SCR 0156-6402A 0.197 85.6 140.4 SCR 0156-6402B 0.217 86.2 82.1 280.5 261.8 ^b	
SCR 0156-6702A 0.183 57.4 29.7 SCR 0156-6702B 0.177 47.4 45.2 19.3 79.8 ^b	
SCR 0205-6122A 0.184 192.8 [74.6] SCR 0205-6122B ··· ··· ··· ··· ··· ··· a , b	
SCR 0206-6609A 0.181 80.6 101.4 SCR 0206-6609B 0.220 75.9 124.5 107.4 92.6 ^b	
SCR $0246-4935$ A 0.247 72.3 40.0 SCR $0246-4935$ B 0.243 58.0 (31.4) 8.2 145.3 a, b, c	
SCR 0353-6844A 0.232 38.0 53.2 SCR 0353-6844B 0.238 38.1 59.3 13.5 226.4	
SCR 0429-5423A 0.188 49.4 54.4 SCR 0429-5423B 0.170 39.7 \cdots 138.0 115.4 $^{\rm b}$, $^{\rm d}$, WD candidate	at $40.5 \pm 8.1 \mathrm{pc}$
SCR 0454-8045A 0.195 14.2 43.0 SCR 0454-8045B 0.191 13.5 56.5 14.4 189.1	
SCR 0611-7302A 0.188 208.1 65.7 SCR 0611-7302B 0.190 211.4 69.4 101.9 46.1	
SCR 0745-4814A 0.200 174.9 31.4 SCR 0745-4814B 0.201 176.0 25.7 43.7 220.5 b	
SCR 0757-7444A 0.197 50.9 (99.4) SCR 0757-7444B 0.180 48.0 158.5 10.4 311.4 ^b , ^c	
SCR 0853-7705A 0.211 306.7 52.6 SCR 0853-7705B 0.225 293.2 76.2 224.1 99.5	
SCR 0921-7523A 0.291 321.1 62.2 SCR 0921-7523B 0.286 316.3 80.4 14.0 309.5	
SCR 1117-7226A 0.188 275.8 72.2 NLTT 26927 0.204 273.7 52.0 28.8 30.5	
SCR 1229-5738A 0.197 256.6 92.7 SCR 1229-5738B 0.189 262.7 109.8 10.8 215.0 b	

- 19 -

Table 5—Continued

Primary	μ (")	heta (°)	Distance (pc)	Secondary/Tertiary	$\mu \ ('')$	heta (°)	Distance (pc)	Separation (")	heta (°)	notes	_
SCR 1246-5328A	0.188	29.0	45.3	SCR 1246-5328B	0.183	25.3	82.1	19.5	298.8		-
SCR 1800-5112A	0.289	226.5		SCR 1800-5112B	0.317	220.3	178.3	4.6	123.7	a , b	
SCR 1804-5541A	0.222	194.4	(47.2)	SCR 1804-5541B	0.198	201.7	163.4	18.9	302.6	b c	
SCR 1809-6154A	0.218	253.2	159.3	SCR 1809-6154B	0.201	259.8	163.9	19.3	269.7		
SCR 1816-6615A	0.209	207.1	[448.4]	SCR 1816-6615B						a, b	
SCR 1902-7550A	0.303	168.8	75.9	P 1248-2	0.286	168.5	111.7	20.3	129.4	b	
SCR 1912-4910A	0.229	187.7	35.8	SCR 1912-4910B	0.254	185.5	42.3	20.9	262.8		
SCR 1917-4915A	0.216	200.3	48.2	P 3221-2	0.212	200.8	81.8	44.0	131.6	b	
SCR 1953-5037A	0.181	144.3	31.6	SCR 1953-5037B	0.171	142.9	45.0	82.5	188.8	b	
SCR 1958-8000A	0.183	149.1	(61.3)	SCR 1958-8000B	0.192	145.8	(133.4)	6.7	258.7	$^{\rm b}$, $^{\rm f}$, without I A at 81pc and B at 128pc	
SCR 2032-4948A	0.265	179.0	75.3	SCR 2032-4948B	0.270	182.4	[900.1]	8.8	213.1	$^{\mathrm{b}}$, $^{\mathrm{d}}$, WD candidate at 48.7 \pm 9.7pc	
SCR 2036-6454A	0.197	146.0	72.7	SCR 2036-6454B	0.190	153.3	88.2	35.3	72.5		
SCR 2057-6358A	0.187	139.9	[102.0]	SCR 2057-6358B						a, b	
				SCR 2057-6358C	0.130	138.7	46.7	261.5	121.6	b	
SCR 2100-5804A	0.186	117.6	80.5	SCR 2100-5804B	0.181	116.1	147.0	16.4	300.7	b	1
SCR 2112-5428A	0.209	95.3	35.6	SCR 2112-5428B	0.152	117.0	13.5	15.3	60.6	b	
SCR 2218-5310A	0.190	95.3	(61.1)	SCR 2218-5310B	0.191	95.9	96.6	35.2	142.1	c	
SCR 2241-6119A	0.184	124.0	23.2	SCR 2241-6119B	0.162	117.6	27.8	9.6	211.2	b	
SCR 2255-5120A	0.335	227.1	69.7	SCR 2255-5120B	0.263	228.9	112.6	17.4	359.3	b	
SCR 2333-7923A	0.394	101.4	[183.1]	SCR 2333-7923B	0.388	100.0	[216.2]	11.2	123.0	g	
SCR 2335-6433A	0.196	103.1	(24.5)	SCR 2335-6433B	0.196	99.1	57.5	22.4	25.9	h	
SCR 2353-8204A	0.216	66.9	(26.8)	SCR 2353-8204B	0.209	68.4	54.2	34.5	181.9	h	

^aDistance estimate unreliable when listed [in brackets]; if distance not given BRI photometry not available

^bCompanion not detected during automated search but noticed to be a common proper motion companion during visual inspection

^cFewer than 6 relations, therefore distance estimate unreliable (in parenthesis); Hipparcos distance given in notes when available

^dWhite dwarf candidate with unreliable distance when listed [in brackets]

^eNo 2MASS photometry available for companion

^fI photometry suspect, therefore distance unreliable (in parenthesis)

^gSubdwarf candidate with unreliable distance listed [in brackets]

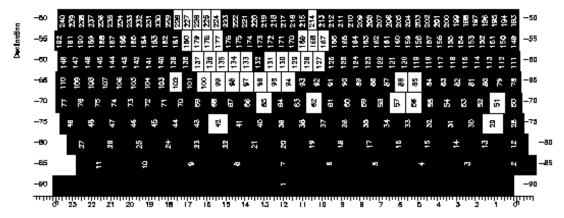
^hDistance estimate unreliable (in parenthesis), because primary is likely a double

Table 6. Distance Estimate Statistics for New SCR Systems.^a

Proper motion	$d \le 10 \ pc$	$10~{\rm pc} < {\rm d} \leq 25~{\rm pc}$	d > 25 pc
$\begin{array}{c} \mu \geq 1.00 \ \mathrm{yr}^{-1} \\ 1.00 \ \mathrm{yr}^{-1} > \mu \geq 0.80 \ \mathrm{yr}^{-1} \\ 0.80 \ \mathrm{yr}^{-1} > \mu \geq 0.80 \ \mathrm{yr}^{-1} \\ 0.80 \ \mathrm{yr}^{-1} > \mu \geq 0.80 \ \mathrm{yr}^{-1} \\ 0.80 \ \mathrm{yr}^{-1} > \mu \geq 0.80 \ \mathrm{yr}^{-1} \\ 0.80 \ \mathrm{yr}^{-1} > \mu \geq 0.80 \ \mathrm{yr}^{-1} \\ 0.80 \ \mathrm{yr}^{-1} > \mu \geq 0.80 \ \mathrm{yr}^{-1} \\ 0.80 \ \mathrm{yr}^{-1} > \mu \geq 0.80 \ \mathrm{yr}^{-1} \\ 0.80 \ \mathrm{yr}^{-1} > \mu \geq 0.80 \ \mathrm{yr}^{-1} \end{array}$	$ 2 + 0 + 0 \\ 0 + 0 + 0 \\ 0 + 1 + 0 \\ 1 + 1 + 0 \\ 0 + 0 + 2 $	0+0+03+0+04+7+08+16+00+0+29	2 + 4 + 0 $2 + 1 + 0$ $25 + 23 + 0$ $95 + 93 + 0$ $0 + 0 + 1542$
7 Total	3 + 2 + 2	15 + 23 + 29	124 + 121 + 1542

 $^{\mathrm{a}}$ Entire SCR sample excluding white dwarf candidates and new common proper motion companions to known objects noticed by eye; the first number from Paper XII, second number from Paper XV, third number from this paper

- Fig. 1.— Plate coverage of the sky included in the MINIMO search. White boxes indicate plates that were excluded, primarily due to crowding in the Galactic Plane, LMC, and SMC, or because of an insufficient spread in plate epochs.
- Fig. 2.— Hit Rate percentage of true proper motion objects (real proper motion objects / total candidates extracted) for the entire SCR sample having $\mu \geq 0''.18 \text{ yr}^{-1}$ south of -47° . Horizontal bars show the proper motion bins adopted, while vertical lines delineate the three individual SCR samples MOTION, SLOWMO and MINIMO.
- Fig. 3.— Comparison of NLTT, Hipparcos, and SCR proper motions and position angles. The solid line indicates perfect agreement. Note that proper motion data for NLTT is quantized south of -45° .
- Fig. 4.— Color-apparent magnitude diagram for SCR systems (open circles) and known systems (small points) with 0'.40 yr⁻¹ > $\mu \ge 0$ '.18 yr⁻¹ from $-90^{\circ} > \delta \ge -47^{\circ}$. Data points below $R_{59F} J = 16.5$ are CPM companions noticed during the blinking process.
- Fig. 5.— Reduced proper motion diagram for SCR systems (open circles) and known systems (small points) with 0'.40 yr⁻¹ > $\mu \ge 0'$.18 yr⁻¹ from $-90^{\circ} > \delta \ge -47^{\circ}$. The arbitrary dotted line separates the white dwarfs from the subdwarfs. Triangles denote previously known white dwarfs.
- Fig. 6.— Comparison of proper motions for components in CPM systems. Proper motions from the automated SCR search are denoted by filled circles and proper motions manually obtained through SuperCOSMOS are denoted by open circles. The solid line indicates perfect agreement between the two and the dashed lines represent conservative limits of 0.020 yr⁻¹ based on our uncertanties.
- Fig. 7.— Comparison of position angles for components in multiple CPM systems. Position angles from the automated SCR search are denoted by filled circles and position angles manually obtained through SuperCOSMOS are denoted by open circles. The solid line indicates perfect agreement between the two and the dashed lines represent conservative limits of 5.0 degrees based on our uncertanties.
- Fig. 8.— Sky distribution of SCR systems with $\mu \geq 0$. 18 yr⁻¹. Open circles denote SCR discoveries from this paper and filled circles indicate SCR discoveries from past papers. The curve represents the Galactic plane.



Right Assension

